Aquatic Toxicology 214 (2019) 105265

Contents lists available at ScienceDirect

Aquatic Toxicology

journal homepage: www.elsevier.com/locate/aqtox

Chronic exposure of the freshwater alga *Pseudokirchneriella subcapitata* to five oxide nanoparticles: Hazard assessment and cytotoxicity mechanisms

Cátia A. Sousa[a,b,c], Helena M.V.M. Soares[c,*], Eduardo V. Soares[a,b,*]

[a] Bioengineering Laboratory-CIETI, ISEP-School of Engineering, Polytechnic Institute of Porto, rua Dr António Bernardino de Almeida, 431, 4249-015, Porto, Portugal
[b] CEB-Centre of Biological Engineering, University of Minho, Campus de Gualtar, 4710-057, Braga, Portugal
[c] REQUIMTE/LAQV, Departamento de Engenharia Química, Faculdade de Engenharia, Universidade do Porto, rua Dr Roberto Frias, s/n, 4200-465, Porto, Portugal

ARTICLE INFO

Keywords:
Metabolic (esterase) activity
Microalga
Nanomaterials
Nanotoxicity
Oxidative stress
Photosynthesis

ABSTRACT

The increasing use of nanoparticles (NPs) unavoidably enhances their unintended introduction into the aquatic systems, raising concerns about their nanosafety. This work aims to assess the toxicity of five oxide NPs (Al_2O_3, Mn_3O_4, In_2O_3, SiO_2 and SnO_2) using the freshwater alga *Pseudokirchneriella subcapitata* as a primary producer of ecological relevance. These NPs, in OECD medium, were poorly soluble and unstable (displayed low zeta potential values and presented the tendency to agglomerate). Using the algal growth inhibition assay and taking into account the respective 72 h-EC_{50} values, it was possible to categorize the NPs as: toxic (Al_2O_3 and SnO_2); harmful (Mn_3O_4 and SiO_2) and non-toxic/non-classified (In_2O_3). The toxic effects were mainly due to the NPs, except for SnO_2 which toxicity can mainly be attributed to the Sn ions leached from the NPs. A mechanistic study was undertaken using different physiological endpoints (cell membrane integrity, metabolic activity, photosynthetic efficiency and intracellular ROS accumulation). It was observed that Al_2O_3, Mn_3O_4 and SiO_2 induced an algistatic effect (growth inhibition without loss of membrane integrity) most likely as a consequence of the cumulative effect of adverse outcomes: i) reduction of the photosynthetic efficiency of the photosystem II (Φ_{PSII}); ii) intracellular ROS accumulation and iii) loss of metabolic activity. SnO_2 NPs also provoked an algistatic effect probably as a consequence of the reduction of Φ_{PSII} since no modification of intracellular ROS levels and metabolic activity were observed. Altogether, the results here presented allowed to categorize the toxicity of the five NPs and shed light on the mechanisms behind NPs toxicity in the green alga *P. subcapitata*.

1. Introduction

In the emerging field of nanotechnology, the nanoparticles (NPs) exhibit unique physical and chemical properties due to their limited size (< 100 nm). Metal(loid) oxide (MOx) NPs, such as aluminium oxide (Al_2O_3), indium oxide (In_2O_3), manganese oxide (Mn_3O_4), silicon dioxide (SiO_2) and tin(IV) oxide (SnO_2) can be used in a wide range of fields, such as optics, electric and electronics, medical imaging, cosmetics, plastic production, ceramics, fuel additives and aerospace industry (Andreescu et al., 2012; Laurent et al., 2018; Nanotech, 2015; Tian et al., 2013; Vranic et al., 2019); for a more detailed description of the possible uses of these NPs, the reader can consult the table S1.

The safe use of nanotechnology, on an industrial scale, requires a careful evaluation of the potential environmental and human health risks that can result from the release of NPs into the environment. The increasing use of NPs inevitably intensifies their unintended introduction into the environment. Thus, the toxicity data of NPs are very important for the risk evaluation in aquatic environments. Algae, as primary producers, represent the base of food chain (first trophic level). Therefore, due to their ecological importance, universal distribution and sensitivity to a wide variety of toxicants, the alga *Pseudokirchneriella subcapitata* have been used in the assessment of toxicity (algal growth inhibition assay) (Geis et al., 2000; OECD, 2011; US-EPA, 2002).

Studies carried out in the last decade evidence that NPs, including MOx NPs can cause toxic effects. In this context, it was described that Al_2O_3 NPs caused growth inhibition and reduction of chlorophyll content in the green algae *Chlorella* sp. and *Scenedesmus* sp. (Sadiq et al., 2011) and in the red alga *Porphyridium aerugineum* Geitler (Karunakaran et al., 2015). SiO_2 NPs inhibited the growth of the marine algae *Dunaliella tertiolecta* (Manzo et al., 2015); similarly, growth inhibition, reduction of chlorophyll and protein content in *Porphyridium aerugineum* Geitler exposed to SiO_2 NPs was described (Karunakaran et al., 2015). Aruoja et al. (2015) showed that Al_2O_3, Mn_3O_4 and SiO_2

* Corresponding authors.
E-mail addresses: hsoares@fe.up.pt (H.M.V.M. Soares), evs@isep.ipp.pt (E.V. Soares).

https://doi.org/10.1016/j.aquatox.2019.105265
Received 22 April 2019; Received in revised form 22 July 2019; Accepted 25 July 2019
Available online 26 July 2019
0166-445X/

NPs caused growth inhibition of the alga *P. subcapitata*. Nonetheless, Al_2O_3, In_2O_3 and SnO_2 NPs seem to be nontoxic to the marine diatom *Skeletonema costatum* (Ng et al., 2015).

Despite the commercial importance of metal(loid)-based NPs, a limited information can be found in the literature regarding the potential ecotoxicity of the NPs studied, namely: i) the hazard evaluation; ii) the understanding of the mechanisms behind NPs toxicity. In this sense, this work aimed to assess the ecotoxicity (assessment and categorization of NP hazards) of five NPs (Al_2O_3, In_2O_3, Mn_3O_4, SiO_2 and SnO_2) by means of the environmentally relevant organism *P. subcapitata*, using algal growth inhibition assay. In addition, physico-chemical properties of NPs [hydrodynamic size, zeta potential, agglomeration, dissolution and abiotic production of reactive oxygen species (ROS)] were characterized in order to understand their toxic impact. With regard to shed light on the mechanisms behind NP toxicity, the key responses at subcellular level, of the freshwater alga *P. subcapitata* were evaluated as potential markers of cytotoxicity; thus, plasma membrane integrity, intracellular accumulation of ROS, metabolic activity and photosynthetic performance was assessed in algal cells chronic exposed (72 h) to different NP concentrations. To our knowledge, this is the first work that provides a comprehensive study of the impact of Al_2O_3, In_2O_3, Mn_3O_4, SiO_2 and SnO_2 NPs on the physiology of the microalga *P. subcapitata*. This work contributes to the systematic characterization of the potential pollutant hazards of MOx NPs in the aquatic environment.

2. Material and methods

2.1. Preparation of nanoparticles stock suspensions

The following NPs were used: Al_2O_3 (< 50 nm), In_2O_3 (< 100 nm); Mn_3O_4 (< 30 nm), SiO_2 (< 20 nm) and SnO_2 (< 100 nm), with a purity ≥99.1%. All NPs were purchased from Sigma-Aldrich (St. Louis, MO, USA), except for Mn_3O_4 NPs, which were obtained from abcr GmbH (Karlsruhe, Germany).

Stock suspensions of 0.5 g L^{-1} of the different NPs (or 1 g L^{-1} in the case of In_2O_3 NPs) were prepared in deionized water; subsequently, NPs were shaken, sonicated in a 80–160 W ultrasonic bath (Bandelin, Sonorex RK 100) for 15 min and sterilized under an ultraviolet light (253.7 nm), using a Toshiba 15 W lamp (Ref: Toshiba GL 15), for 30 min. The stock suspensions of NPs were stored up to one month, at 4 °C, in the dark. Before each experiment, the suspensions were shaken and sonicated for 15 min.

2.2. Characterization of NPs in aqueous suspension

The characterization of the NPs was performed in OECD algal medium or in water in the absence of algal cells, under the same conditions of the assays with algae (as described below; Section 2.4).

The hydrodynamic size was evaluated by dynamic light scattering (DLS) using a polystyrene cuvette (DTS0012) and zeta potential was evaluated using a folded capillarity cell (DTS1070), at 25 °C, in a Zetasizer Nano ZS (Malvern Instruments, UK) with Zetasizer software (version 7.11). For this purpose, the NPs were suspended at a concentration corresponding to 72 h-EC_{50} values (see Section 2.4); In_2O_3 NPs were suspended at 100 mg L^{-1}.

The stability of the NPs was studied by measuring the metal(loid)s dissolved from the NPs. Thus, the NPs were suspended in water or OECD medium at a concentration corresponding to 72 h-EC_{50} values (see Section 2.4) or at 100 mg L^{-1}. After 72 h of incubation, samples were taken, centrifuged at 20,000 x*g* for 30 min at 25 °C and the supernatants carefully removed. The metal(loid)s were quantified by atomic absorption spectroscopy with flame atomization (AAS-FA) (Mn), with electrothermal atomization (AAS-EA) (Al, In and Sn) or by inductively coupled plasma – optical emission spectrometry (ICP-OES) (Si) in an Analytik Jena novAA 350, a Perkin Elmer AAnalyst 600 spectrometer or a Thermo Fisher iCAP 7000 series spectrometer, respectively. The total concentration of Al, In, Mn or Sn present in the NPs was evaluated after total digestion of the NPs with aqua regia. For this purpose, 2.0 mL of NP suspensions were placed in contact with 4.0 mL of aqua regia (1.0 mL nitric acid [13.4 mol L^{-1}] and 3.0 mL hydrochloric acid [12.2 mol L^{-1}]) for 1 h; subsequently, samples were filtered through a 0.45-µm-pore-size membrane and quantitatively transferred to 10 mL volumetric flasks, appropriately diluted and metal content determined by AAS-FA.

NP agglomeration was evaluated through a sedimentation assay, as previously described (Sousa et al., 2018). With this aim, NPs were suspended in OECD medium at 100 mg L^{-1} and agitated at 150 rpm for 72 h, at 25 °C. For a given incubation time, samples were withdrawn and placed in 3 mL cuvettes. The turbidity change of the samples was monitored, spectrophotometrically (optical density at 600 nm, OD_{600}) over a period of 60 min. The percentage of initial OD_{600} after 60 min was calculated according to Eq. (1):

$$\% \text{ of initial } OD_{600} \text{ after 60 min} = (OD_t/OD_i) \times 100 \quad (1)$$

where OD_t is the OD_{600} after 60 min of settling and OD_i is the OD_{600} at zero time. The % of initial OD_{600} after 60 min calculated was plotted against the incubation time of NPs.

2.3. Strain, medium and culture conditions

In this study, the freshwater green alga *Pseudokirchneriella subcapitata* (strain 278/4) was used. The alga was obtained from the Culture Collection of Algae and Protozoa (CCAP), UK, and maintained in OECD agar medium (OECD, 2011).

The pre-cultures were prepared, weekly, by inoculating 40 mL of OECD medium, in 100 mL Erlenmeyer flasks, with a loop of algae. Cells were incubated for 3 days, at 25 °C, in an orbital shaker at 100 rpm, under continuous “natural white” light-emitting diodes (LEDs) with a colour temperature of 4000–4200 K and an intensity of 4000 lx at the surface of the flasks.

The cultures were obtained by inoculating the algal cells, from the pre-cultures, at 5×10^4 cells mL^{-1} in 100 mL of OECD medium, in 250 mL Erlenmeyer flasks; algal cells were incubated for 48 h under the same conditions described for the pre-cultures. After growth, algal cells were harvested by centrifugation (2,500 × *g* for 5 min) and suspended in deionized water.

2.4. Algal bioassays

Concentration-response curves of Al_2O_3, In_2O_3, Mn_3O_4, SiO_2 or SnO_2 NPs were performed using the freshwater alga growth inhibition test (OECD, 2011). The toxicity caused by the respective metal ions (in the case of Al_2O_3, In_2O_3, Mn_3O_4 and SnO_2 NPs) was compared. Similar experiences with Si (a metalloid) could not be done since the chemical behaviour of this element is different from the metals (Hirner and Flaßbeck, 2005); the dissolution of SiO_2 in water, originates as the formation of orthosilicic acid (Iler, 1978). Algal cells in exponential phase of growth (2 days), at 5×10^4 cells mL^{-1}, were exposed (at least) to seven concentrations of toxicants, arranged in a geometric series, in OECD medium. The assays were conducted in 250 mL Erlenmeyer flasks, at a final volume of 100 mL. As control, algal cells were grown in the absence of toxicant. The metals stock solutions used were: $Al(NO_3)_3$ (1000 mg L^{-1}, Merck, Darmstadt, Germany), $In(NO_3)_3$ (1000 mg L^{-1}, Sigma-Aldrich), $MnCl_2$ (2000 mg L^{-1}, Merck) and $SnCl_4$ (1000 mg L^{-1}, Merck). After 72 h of incubation, under the conditions described above, algal cell concentrations were determined using an automated cell counter (TC10, Bio-Rad), image analysis-based. The test endpoint was biomass yield, defined as biomass (number of cells mL^{-1}) at the end of the exposure period (72 h) minus the biomass at the start of the exposure period (OECD, 2011). The 72 h-EC_{10}, EC_{25}, EC_{50}, EC_{75} and EC_{90}

values, which represent the toxicant concentration that induces an inhibition of 10, 25, 50, 75 or 90%, respectively, of algal growth after 72 h, when compared with control, were determined using a linear interpolation method (TOXCALC version 5.0.32, Tidepool Scientific Software, McKinleyville, CA, USA).

P. subcapitata algal cells were also exposed to three concentrations (corresponding to the previously calculated 72 h-EC_{10}, 72 h-EC_{50}, and 72 h-EC_{90} values) of each nanoparticle for 72 h. For concentration-response curve determination, the assays were carried out as described above. After exposure to NPs, algal cells were centrifuged at 2,500 x *g* for 5 min and, subsequently re-suspended in fresh OECD medium at a final concentration of 3×10^6 cells mL^{-1} (for photosynthetic performance assay; see Section 2.7) or 1×10^6 cells mL^{-1} (for membrane integrity and ROS production assays) or 5×10^5 cells mL^{-1} (for metabolic activity). The use of different cell concentrations was a consequence of the optimization of conditions, previously performed for each determination. The specific works on which the conditions were originally described can be found below (Sections 2.6 and 2.7).

2.5. The entrapment assay of algae

The dispersibility of NP-alga hetero-agglomerates was evaluated using an algal entrapment-test. A known concentration of algal cells (1×10^5 or 3×10^6 cells mL^{-1}, which corresponded to the minimal and maximal cell concentrations achieved at the end of EC_{10} and EC_{90} assays, respectively) was incubated, in the same conditions of algal bioassays, with the highest NP concentration tested; for these NP concentrations, no algal growth was observed. After 72 h of incubation, the algal-NP suspensions were vortexed and dispersed cell concentrations were determined using an automated cell counter. The reduction of algal cells in suspension (in percentage), which corresponded to the algae entrapped in the NP agglomerates, was determined considering the initial algal cell concentration as reference.

2.6. Staining procedures

SYTOX Green (SG) staining was used to evaluate the impact of NPs on plasma membrane integrity of algal cells (Machado and Soares, 2012). For this purpose, algal cells were exposed to NPs, at a concentration which corresponded to the 72 h-EC_{90} value (for each NP), for 72 or 144 h. Subsequently, algae at 1×10^6 cells mL^{-1} were stained with 0.5 μmol L^{-1} SG (Molecular Probes, Invitrogen), for 20 min in the dark at 25 °C. As positive control (cells with disrupted plasma membrane; SG positive cells), algae were heat-treated (65 °C, 60 min) in a water bath and subsequently stained with SG. Cells were observed in a Leica DLMB epifluorescence microscope (Wetzlar GmbH, Germany), equipped with an HBO-100 mercury lamp and the GFP filter set from Leica. For each experiment and condition tested, two samples of ~200 cells were analysed in randomly selected microscope fields.

The metabolic activity of algal cells was evaluated using fluorescein diacetate (FDA). After treatment with NPs, 5×10^5 cells mL^{-1} in OECD medium were stained with 20 μmol L^{-1} FDA for 40 min in the dark at 25 °C, as previously described (Machado and Soares, 2013). The assays were carried out in quintuplicate in 96-well flat microplates (Orange Scientific). Fluorescence intensity (in relative fluorescent units, RFUs) was measured in a microplate reader at a fluorescence excitation wavelength of 485/14 nm and an emission wavelength of 535/25 nm. Fluorescence was corrected by subtracting cell, culture medium and dye autofluorescence. The results were expressed as the ratio of fluorescence in the cells exposed to MOx NPs/fluorescence in the control (non-treated cells).

The intracellular accumulation of ROS was quantitatively assessed using the fluorescent probe 2′,7′-dichlorodihydrofluorescein diacetate (H_2DCFDA; Sigma-Aldrich) (Machado and Soares, 2016). Control and cells treated with NPs, at 1×10^6 cells mL^{-1}, were mixed with 10 μmol L^{-1} H_2DCFDA, dispensed in quintuplicate in a 96-well microplate and incubated in the dark for 90 min at 25 °C. Fluorescence was measured and corrected and the results expressed as described above for metabolic activity.

The production of ROS by NPs in abiotic conditions (in the absence of cells) was also quantified by deacetylation of the probe H_2DCFDA to H_2DCF, as previously described (Aruoja et al., 2015). NPs (at a concentration corresponding to the respective 72 h-EC_{90} value) were incubated for 72 h in OECD medium in the same conditions described above for the assays with algal cells. Then, 100 μL of samples were collected and incubated with 100 μL of 52 μmol L^{-1} H_2DCF, placed in quintuplicate in a 96-well microplate and incubated in the dark for 45 min at 25 °C. A blank and a positive control were prepared by replacing the sample by equal volume of OECD medium or 52 μmol L^{-1} H_2O_2, respectively, as previously described (Sousa et al., 2018). Fluorescence was measured and corrected as described above for metabolic activity. The results were presented as the ratio of fluorescence of the assay/fluorescence of the blank.

2.7. Algal photosynthetic performance determination

Photosynthetic performance of Photosystem II (PSII) of algal cells was evaluated trough the determination of the effective photochemical quantum yield of PS II (Φ_{PSII}) by pulse amplitude modulated (PAM) fluorescence assay, using a chlorophyll fluorometer (Walz, JUNIOR-PAM), as previously described (Sousa et al., 2018). Algal cells not exposed (control) or exposed to NPs were suspended in OECD medium at 3×10^6 mL^{-1}. After a dark adaptation for 30 min the minimal fluorescence was measured. Then, the maximum fluorescence was determined by exposing the cells for 600 ms to a blue LED saturation pulse of 10,000 μmol m^{-2} s^{-1} light intensity and a measuring beam of 5 Hz. Φ_{PSII} was automatically calculated using the WinControl software (version 3.25), according to Eq. (2) (Genty et al., 1989):

$$\Phi_{PSII} = (F'_m - F')/F'_m \quad (2)$$

where F'_m is the maximal fluorescence level (when PSII reaction centres are closed by a strong light pulse) and F' is the fluorescence level shortly before a strong light pulse.

The results were expressed as a ratio of the values in assay (cells treated with the MOx NPs) and the values in control.

2.8. Microphotographs

Nanoparticle suspensions were observed by phase-contrast microscopy. Algal cells in the presence of NPs were also microscopically observed by phase-contrast and fluorescence microscopy using an I3 filter set from Leica. All images were acquired with a Leica DC 300 F camera, using a N plan ×100 objective, and were processed using Leica IM 50-Image manager software.

2.9. Reproducibility of the results and statistical analysis

The hydrodynamic size and zeta potential measurements were performed one time in duplicate; in each measurement, ten repetitions were considered. The other studies were repeated at least three times in duplicate ($n \geq 6$). The data are presented as mean values ± standard deviations (SD). The mean values were subjected to one-way ANOVA, followed by Tukey-Kramer multiple comparison method; P values < 0.05 were considered statistically significant.

3. Results

3.1. Physico-chemical characterization of NP suspensions

The NP suspensions were characterized in the algal (OECD) medium; for comparative purposes, the same analysis was performed in

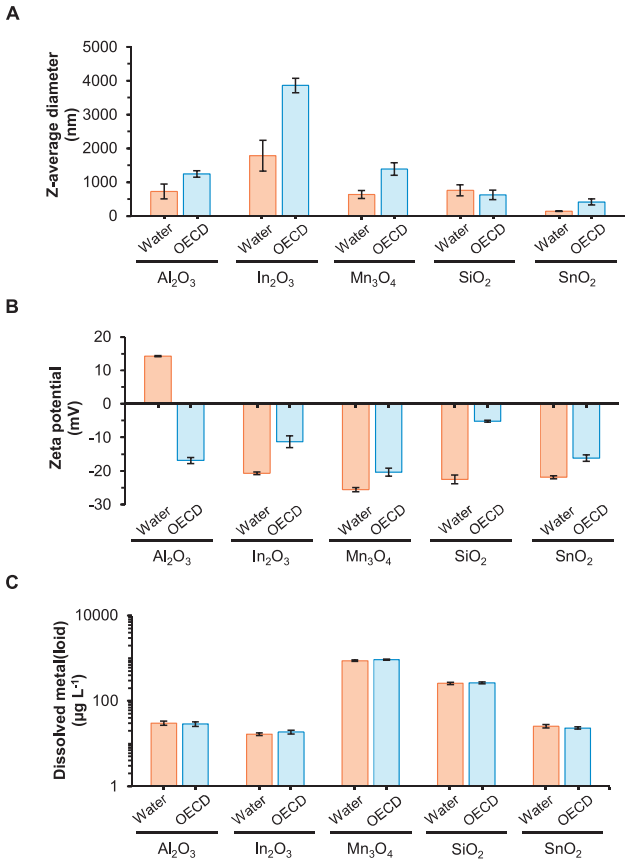

Fig. 1. Physicochemical characterization of the nanoparticles in water and in OECD medium. NPs were suspended in water or OECD medium, at 72 h-EC_{50} values, except for In_2O_3 NPs, which were suspended at 100 mg L^{-1}. A and B – Z-average diameter and zeta potential, respectively, at 0 h (immediately after suspension of the NPs). C – Dissolved metal(loid)s from the NPs at 72 h. The data represent the mean values; standard deviations are presented as vertical error bars. The hydrodynamic size and zeta potential measurements were performed one time in duplicate; in each measurement, ten repetitions were considered. NP solubility experiments were carried out at least three times in duplicate ($n \geq 6$).

deionized water.

The hydrodynamic (Z-average) diameter of the NPs in suspension as well as the zeta potential was determined after the preparation of the suspensions (0 h). Z-average diameter of the NPs, in OECD medium, ranged between 418 and 3859 nm while in water it ranged between 145 and 1785 nm (Fig. 1A). Since all NPs, when in powder, had a nominal size of < 100 nm, these results showed that the NPs agglomerated almost instantaneously after suspension in aqueous solution. The agglomeration of all NPs studied, increased over the time, in OECD medium, as can be seen from the sedimentation profiles of the NPs (Fig. S1). The microscopic observation of NPs suspensions, after 72 h of incubation, confirmed the formation of agglomerates in all NPs studied (Fig. S2). This effect was particularly evident for Mn_3O_4 and In_2O_3 NPs, where agglomerates could be detected with the naked eye (Fig. S3).

The zeta potential of NPs, in both media, had negative values (between −5 and −25 mV), except for Al_2O_3 NPs in water, which presented a value of +14 mV (Fig. 1B). In a general way, the magnitude of the zeta potential values was lower in OECD medium comparatively to water (Fig. 1B).

The solubility of all NPs, after 72 h of incubation, at a concentration corresponding to 72 h-EC_{50} values, was similar in OECD medium and deionized water (Fig. 1C). For comparative purposes, the NPs were suspended in OECD medium at 100 mg L^{-1}. Mn_3O_4 NPs were the most soluble; for these NPs, after 72 h of incubation, the amount of Mn ions released was 1000 µg L^{-1} (Fig. S4), which corresponded to a NP solubilisation of 4.2%. The Si released from NPs was 452 µg L^{-1} (Fig. S4), which corresponded to a NPs solubilisation of ~1%. The other NPs studied displayed a much lower solubility (≤0.15%).

The suspension of NPs in OECD medium did not modify substantially the pH, in the presence or absence of algae, during the incubation period of 72 h (Table S2).

3.2. Hazard ranking of NPs

In the last decade, there has been a rapid advance of nanotechnology in terms of developing of new nanomaterials along with their commercial applications, which makes the aspect of nanosafety particularly important. In this context, the potential toxic impact of Al_2O_3, In_2O_3, Mn_3O_4, SiO_2 and SnO_2 NPs was evaluated using the microalga *P. subcapitata* through the OECD algal growth inhibition test (OECD, 2011). For comparative purposes, the toxicity of the corresponding metal ions was also studied. Hence, *P. subcapitata* cells were exposed to a series of geometric concentrations of the toxicants and the corresponding concentration-response curves (expressed as % of growth inhibition) were constructed (Fig. 2). Among the NPs studied, SnO_2 was the most toxic with a 72 h-EC_{50} value of 2.1 mg L^{-1} (Table S3). Considering the 72 h-EC_{50} values (Table S3), the decreasing order of toxicity of the NPs studied is: $SnO_2 > Al_2O_3 > Mn_3O_4 > SiO_2 > In_2O_3$. Related to the metal ions present in the NPs, the decreasing order of toxicity is: $Sn^{4+} > In^{3+} > Al^{3+} > Mn^{2+}$ (Table S3). A detailed comparison of the NPs hazards, considering the respective 72 h-EC_{10}, EC_{25}, EC_{50}, EC_{75} and EC_{90} values is presented in the table S3.

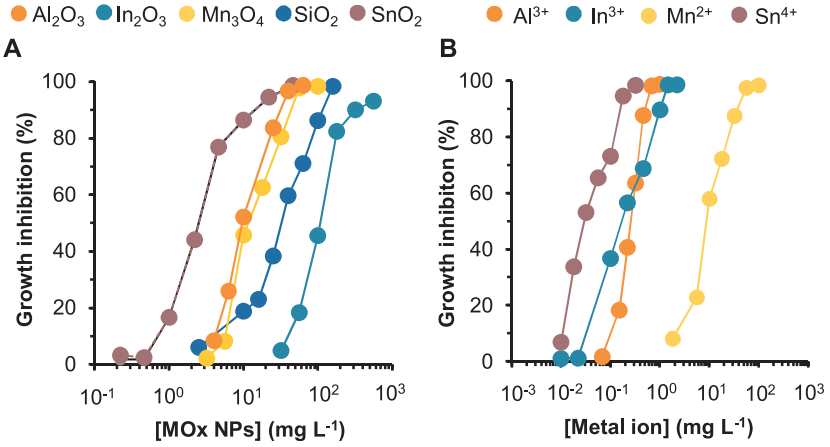

Fig. 2. Concentration-response curves of the nanoparticles or the respective metal ions. A and B – Algal cells of *P. subcapitata* exposed to NPs or to metal ions, respectively, in OECD medium, for 72 h. The data are presented as mean values from at least three independent experiments performed in duplicate ($n \geq 6$); standard deviations are presented (vertical error bars).

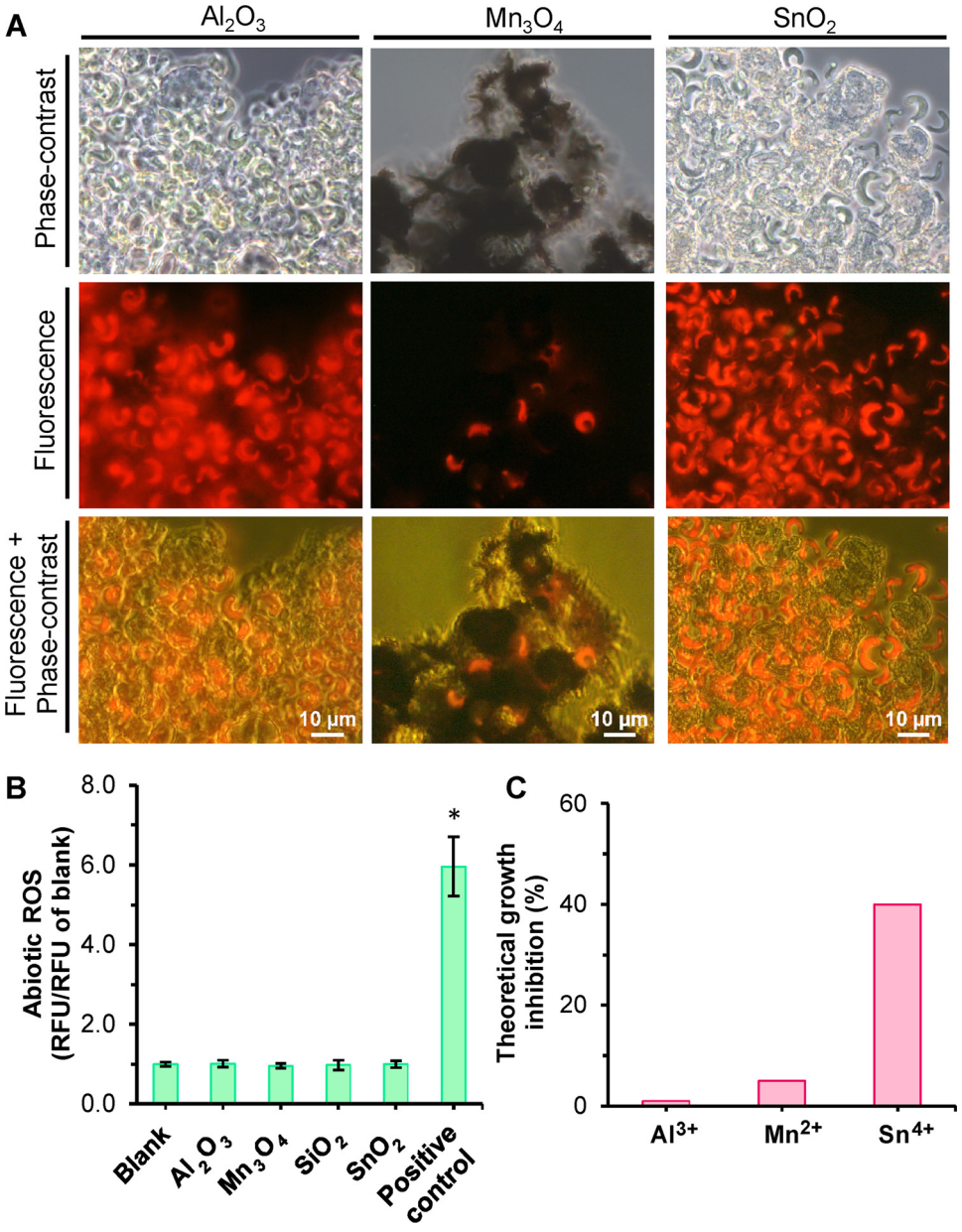

Fig. 3. Possible toxic mechanisms of the nanoparticles. A – Microscopic visualization of algal-NP agglomerates. Algal cells were incubated with NPs for 72 h, at a concentration corresponding to 72 h-EC_{90} values. B – Evaluation of abiotic ROS production by nanoparticles. NPs were suspended in OECD medium at a concentration corresponding to 72 h-EC_{50} values and incubated for 72 h in the same conditions of the biotic assays. Blank and positive control were prepared by incubating the H_2DCF probe with OECD medium or 26 µmol L^{-1} H_2O_2, respectively. The data represent the mean values from at least three independent experiments performed in duplicate ($n \geq 6$); standard deviations are presented (vertical error bars). The mean values were subjected to one way ANOVA, followed by Tukey-Kramer multiple comparison method; the result with asterisk is significantly different ($P < 0.05$). C- Theoretical algal growth inhibition. Growth inhibition was calculated considering the metal ions released from NPs, at a concentration corresponding to 72h-EC_{50} values, and concentration-response curves of the metals (Fig. 2B).

3.3. How can NPs affect algal growth?

Algal cells can be sequestered due to their co-agglomeration with NPs; in this situation, the access of algae to nutrients, present in the culture medium, can be reduced or impaired. The co-agglomeration of NPs and algal cells was observed for Al_2O_3, Mn_3O_4 and SnO_2 NPs; this effect was particularly notorious at high NPs concentrations (corresponding to 72 h-EC_{90} values). These hetero-agglomerates presented a loose structure appearance (Fig. 3A) and were easily dispersed by simple vortexing of the suspensions. After the stirring of these hetero-agglomerates the proportion of algal cells entrapped in these structures could be estimated. It was < 7% (Table S4). In these algal-NPs agglomerates, it was possible to observe cells inside and at the periphery of the structures as well as in the surrounding medium. For SiO_2 and In_2O_3, only NP homoagglomerates were observed. Together, these observations strongly indicated that the toxicity caused by NPs cannot be attributed to nutritional limitation of algae due to their entrapment by the NPs.

The potential of NPs to generate reactive oxygen species (ROS) and, thus, to induce oxidative stress (OS) and cell toxicity was assessed using the general redox probe H_2DCFDA (Tarpey et al., 2004), previously deacetylated to H_2DCF. Under the concentrations and conditions used, the NPs studied did not generate abiotic ROS (Fig. 3B). Due to the absence of a pro-oxidant effect, it is not plausible that the toxicity observed could be attributed to the abiotic induction of OS, by the NPs, in the surrounding medium.

A common question in nanotoxicology is: what is the contribution of the metal leached from the NPs to the observed toxicity? To answer this question, the theoretical algal growth inhibition was calculated (Fig. 3C), in percentage, taking into account the amount of metals released from the NPs, at a concentration corresponding to 72 h-EC_{50} values (Fig. 1C), and the concentration-response curves of metals ions (Fig. 2B). The comparative analysis of the observed (~50% of algal growth inhibition) with the expected toxicity (considering the metals released from the NPs) revealed that, in the case of Al_2O_3, the toxicity can be attributed to the NPs, since the toxicity that can be attributed to the metals released should be < 1% (Fig. 3C). For Mn_3O_4, the toxicity could be mainly attributed to the NPs, although a small inhibition (< 5%) could be due to the release of Mn ions. On the contrary, the toxicity of SnO_2 NPs can be attributed mainly to the release of Sn ions,

as the Sn dissolved from the NPs should provoke an algal growth inhibition of 40% (Fig. 3C).

3.4. NP toxicity: cellular targets

To further contribute for the elucidation of the modes of toxicity of the NPs, different key cell targets were assessed: cell membrane integrity, metabolic activity, intracellular accumulation of ROS and photosynthetic activity. Therefore, algal cells were exposed for 72 h to different concentrations of NPs, corresponding to 72 h-EC_{10}, EC_{50} and EC_{90} values. With this strategy, algal cells were chronically exposed to a wide range of NP concentrations: from a concentration with a little impact on algal growth (72 h-EC_{10} values) to a concentration where the growth was practically arrested (72 h-EC_{90} values). This study was not conduced with In_2O_3, since these NPs presented a lower toxicity: a 72 h-EC_{50} value > 100 mg L^{-1} (Table S3).

3.4.1. Cell membrane integrity

Cell membrane integrity was evaluated using the fluorescent probe SG. Cells with an intact membrane are not penetrated by SG (SG negative cells) (Machado and Soares, 2012). The exposure of algal cells to the highest NP concentration tested (which corresponded to 72 h-EC_{90} value, for each NP), induced growth arrest (Fig. 4B) without disruption of cell membrane integrity (Fig. 4A). Extending the exposure of algae to NPs up to 144 h (6 days), it was possible to observe the growth stop (Fig. 4B), although the cells remained mostly (> 85%) with an intact cell membrane (SG negative cells) (Fig. 4A). These results indicated that these NPs induced an algistatic effect on *P. subcapitata*.

3.4.2. Metabolic activity

Metabolic activity of algal cells was assessed through the quantification of the esterase activity, using fluorescein diacetate (FDA) as substrate. Esterases, present in metabolically active cells, hydrolyse the FDA, giving cells with green fluorescence. The decrease of green fluorescence has been used as an indicator of the loss of algal metabolic activity (Dorsey et al., 1989; Machado and Soares, 2013).

Algal cells exposed to Al_2O_3, Mn_3O_4 or SiO_2 NPs, at concentrations that inhibit 50 or 90% of algal growth, displayed a reduction of the metabolic activity (Fig. 5A–C). In the case of Al_2O_3 NPs, the reduction of esterase activity was also observed for the lowest concentration tested (4.4 mg L^{-1}). SnO_2 NPs seems not disturb algal metabolic activity, up to 21 mg L^{-1}. In fact, algal cells maintained the esterase activity even when exposed to a concentration that inhibit almost completely cell growth (72 h-EC_{90}) (Fig. 5D).

3.4.3. Intracellular ROS accumulation

The accumulation of ROS by algal cells was monitored with the probe H_2DCFDA, which has been used to detect a broad range of ROS (Tarpey et al., 2004). Algal cells exposed to Al_2O_3, Mn_3O_4 or SiO_2 NPs accumulated ROS (Fig. 6). Since these NPs did not generate ROS in abiotic conditions (Fig. 3B), the levels of ROS exhibited by algal cells were, most likely, intracellularly generated. The oxidative stress experienced by algae was particularly notorious in cells exposed to high Al_2O_3 and Mn_3O_4 NP concentrations (corresponding to 72 h-EC_{90} values) (Fig. 6). Within the NPs studied, the decreasing order of intracellular ROS accumulation was: Mn_3O_4 > Al_2O_3 > SiO_2. SnO_2 NPs, up to 21 mg L^{-1}, did not induce intracellular ROS accumulation (Fig. 6).

3.4.4. Photosynthetic performance

The photosynthetic performance was evaluated using a PAM fluorescence assay. It was possible to observe that algal cells exposed to Al_2O_3, Mn_3O_4, SiO_2 or SnO_2 NPs presented a reduction in the light utilization efficiency of PSII (reduction of photosynthetic efficiency). The decrease of Φ_{PSII} was particularly noticeable in algal cells exposed to high NPs concentrations (Fig. 7). The reduction of Φ_{PSII} is generally seen as a sensitive indicator of stress (Juneau and Popovic, 1999).

4. Discussion

The physicochemical characterization of NPs in aqueous suspension, namely the study of their agglomeration and the stability (solubilisation), is essential to understand their possible toxic effects (Rogers et al., 2010; Wang et al., 2017). The evaluation of the electrokinetic potential of Al_2O_3, In_2O_3, Mn_3O_4, SiO_2 and SnO_2, in OECD algal medium and deionized water, showed that these NPs presented low zeta potential values in aqueous media (Fig. 1B). These results indicated that these NPs are poorly stabilized as consequence of the low electrostatic repulsion between adjacent particles. Particles with low zeta potential tend to agglomerate (Hanaor et al., 2012). Consistent with these data, it was observed that the NPs studied in aqueous media presented a hydrodynamic size between ~150 – 3900 nm (Fig. 1A). In addition, the sedimentability of the NPs increased over the time (Fig. S1), and it was possible to detect NP agglomerates by optical microscopy (Fig. S2) or even with the naked eye (In_2O_3 and Mn_3O_4) (Fig. S3). In line with our data, zeta potential values of the same order of magnitude were described for In_2O_3 (Ahamed et al., 2017; Hasegawa et al., 2012; Jeong et al., 2016), Mn_3O_4 and SiO_2 NPs (Aruoja et al., 2015). Similarly, the agglomeration of the NPs was observed by other authors. For Al_2O_3 NPs, a hydrodynamic size between 392 and 1232 nm in OECD medium was described (Aruoja et al., 2015; Sadiq et al., 2011). In the case of Mn_3O_4 and SiO_2 NPs, Aruoja et al. (2015) described an hydrodynamic size in water of 395 and 148 nm, respectively, and in OECD medium of 920 and 154 nm, respectively.

NPs can exert a toxic impact on algae by different ways such as sequestration of the cells by the NPs (isolating the cells from nutrients), generation of ROS in the external milieu or through the release of metal (loid)s (NPs dissolution) (Aruoja et al., 2015; Rogers et al., 2010; Wang

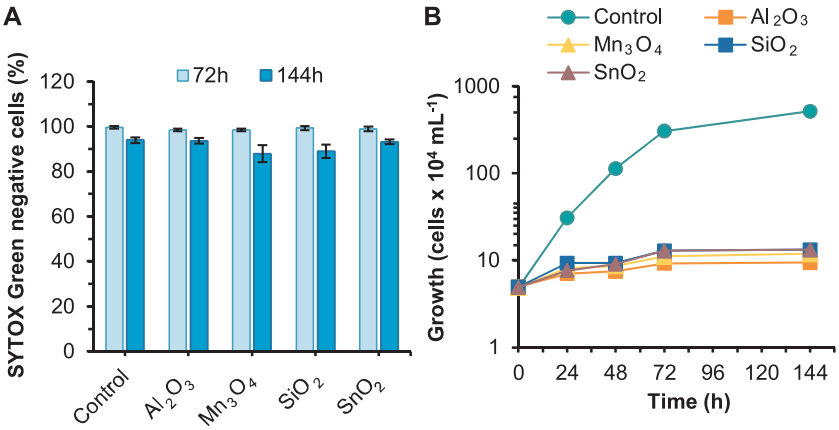

Fig. 4. Effect of nanoparticles on cell membrane integrity and growth of *P. subcapitata*. Algal cells were incubated in OECD medium in the absence (control) or in the presence of NPs, at a concentration corresponding to 72 h-EC_{90} values. A – Cell membrane integrity, evaluated by SYTOX Green exclusion assay, after the exposure of algal cells to NPs for 72 h or 144 h. B – Algal growth. The data are presented as mean values from at least three independent experiments performed in duplicate ($n \geq 6$); standard deviations are presented (vertical error bars). A – Means for 72 h or 144 h are not significantly different ($P < 0.05$; ANOVA).

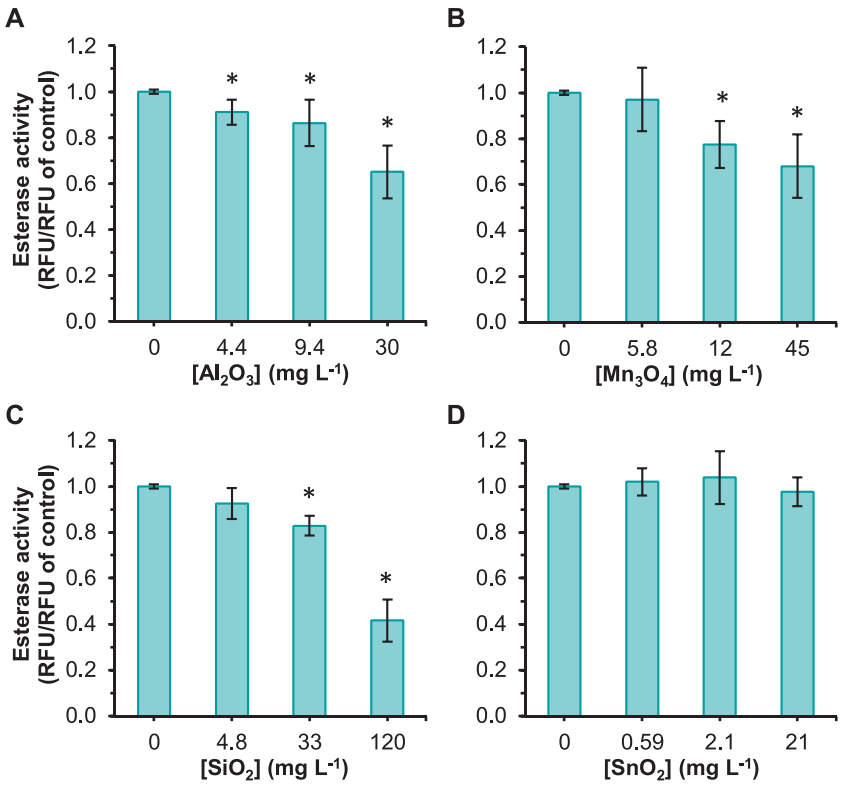

Fig. 5. Influence of the nanoparticles on the metabolic activity of *P. subcapitata*. Algal cells were incubated in the absence or presence of NPs, for 72 h, in OECD medium. Esterase activity was evaluated by the quantification of the hydrolysis of FDA. The data are presented as mean values from at least three independent experiments; in each experiment, five fluorescent readings (in relative fluorescent units, RFUs) were taken ($n \geq 15$). Standard deviations are presented (vertical error bars). Statistical diff ;erences were subjected to ANOVA. The means with asterisks are significantly diff ;erent ($P < 0.05$).

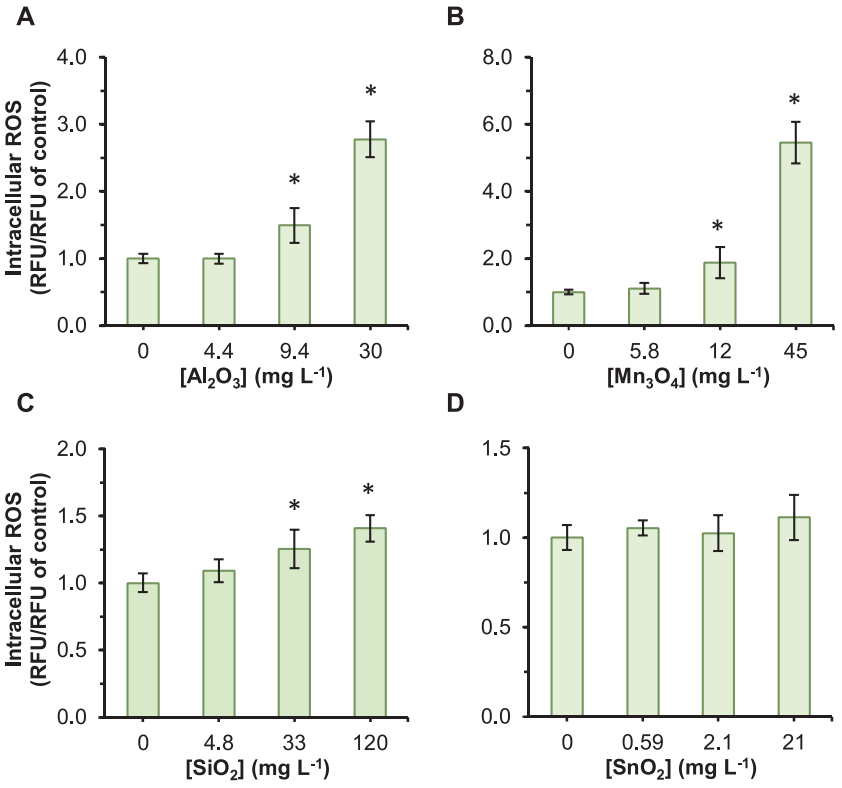

Fig. 6. Evaluation of intracellular ROS accumulation by *P. subcapitata* exposed to nanoparticles. Algal cells were incubated in the absence or presence of NPs, in OECD medium, for 72 h. Intracellular accumulation of ROS was detected using H_2DCFDA. The data are presented as mean values from at least three independent experiments; in each experiment, five fluorescent readings (in relative fluorescent units, RFUs) were performed ($n \geq 15$). Standard deviations are presented (vertical error bars). Statistical diff ;erences were subjected to ANOVA. The means with asterisks are significantly diff ;erent ($P < 0.05$).

et al., 2017). Despite the agglomeration of NPs, it is unlikely that algal entrapment in these structures is the cause of the observed toxicity since alga-NP hetero-agglomerates present a loose structure (Fig. 3A). Reinforcing this possibility, it was shown that after a simple mechanical stirring of algal-NP hetero-agglomerates only < 7% of the algae remained captured in the agglomerates (Table S4).

The quantification of metal(loid)s leached from the NPs (Fig. 1C) revealed that these nanomaterials were poorly soluble in water or OCED medium. A similar solubility was described for Al_2O_3 and Mn_3O_4 NPs in OECD medium (Aruoja et al., 2015). Notwithstanding the lower solubility of SnO_2 NPs, the amount of Sn ions released seems to be the main contributor of the observed toxicity. In fact, SnO_2 NPs presented a

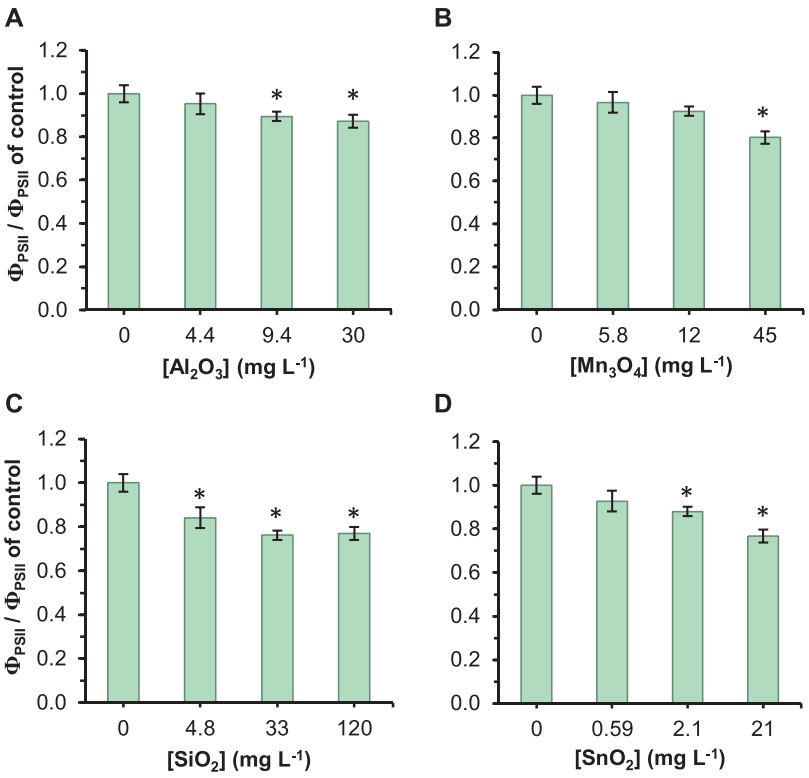

Fig. 7. Photosynthetic performance of algal cells exposed to the nanoparticles. Algal cells were incubated in absence or the presence of NPs, in OECD medium, for 72 h. Effective photochemical quantum yield of PSII (Φ_{PSII}) was assessed using PAM fluorescence assay. The data are presented as mean values from at least three independent experiments, performed in duplicate ($n \geq 6$); standard deviations are presented (vertical error bars). Statistical diff ;erences were subjected to ANOVA. The results with asterisks are significantly diff ;erent ($P < 0.05$).

72 h-EC_{50} value of 2.1 mg L^{-1} (Table S3). When suspended in OECD medium, 2.1 mg L^{-1} SnO_2 NPs released ~23 μg L^{-1} Sn^{4+} (Fig. 1C). According to Sn^{4+} concentration-response toxicity curves (Fig. 2B), this metal concentration (~23 μg L^{-1}) should induce an inhibition of 40% of algal growth (Fig. 3C). In the case of Al_2O_3 and Mn_3O_4 NPs, the ions released should have a minor influence on the observed toxicity (Fig. 3C).

The environmental risk assessment of NPs requires information about their possible adverse effects on aquatic organisms. In the present work, the ecotoxicological hazard of NPs was assessed through their impact on *P. subcapitata* using the OECD algal growth inhibition test. In the framework of EU chemical safety policy, the potential impact of all chemicals manufactured or imported in the EU, above 1 ton per year on aquatic ecosystems has to be characterized (ECHA, 2016). According to the European Commission Directive No 1272/2008, the assessment of risks in the aquatic environment can be made using algal cells and by calculating the EC_{50} values of toxicants through concentration-response curves (EC, 2008). Considering this directive, the impact of pollutants on aquatic systems, based on the EC_{50} values, can be classified as: very toxic (< 1 mg L^{-1}), toxic (1–10 mg L^{-1}), harmful (10–100 mg L^{-1}) and not classified/not harmful (> 100 mg L^{-1}). Therefore, the hazards of the NPs, evaluated through the growth inhibition test of algae, using *P. subc*apitata, can be ranked as follows: SnO_2 (2.1 mg L^{-1}) and Al_2O_3 (9.4 mg L^{-1}) are considered as toxic; Mn_3O_4 (12 mg L^{-1}) and SiO_2 (33 mg L^{-1}) are classified as harmful and In_2O_3 (110 mg L^{-1}) is classified as not classified/not harmful. A similar 72 h-EC_{50} value (34.6 mgL^{-1}) for SiO_2 NPs with *P. subcapitata* was described (Aruoja et al., 2015); however, different EC_{50} values were described for Al_2O_3 (31 mg L^{-1}) and Mn_3O_4 (1.3 mg L^{-1}) (Aruoja et al., 2015); these differences in the EC_{50} values can be due to the use of different alga strains and/or endpoint determination (in the present work: growth yield; literature: fluorescence of algal pigment extract). Higher 72 h-EC_{50} values were described for Al_2O_3 and SiO_2 NPs, evaluated with other algal cells. Thus, for Al_2O_3 NPs, 72 h-EC_{50} values of 39, 45 and 100–300 mg L^{-1} for *Scenedesmus* sp., *Chlorella* sp. (Sadiq et al., 2011) and *Porphyridium aerugineum* Geitler (Karunakaran et al., 2015), respectively, were described. In the case of SiO_2 NPs, a 72 h-EC_{50} value of 1000 mg L^{-1} for the alga *Porphyridium aerugineum* Geitler was reported (Karunakaran et al., 2015). The higher sensitivity of *P. subcapitata* to NPs, compared to other algal genera, reinforces the significance of this alga in the ecotoxicity assessment of freshwaters.

A critical issue regarding to the NP ecotoxicity is related with the knowledge of the toxic modes of action of these nanomaterials. Through photosynthesis, algae convert light energy into chemical energy that can be further used in cellular activities. Thus, it is expected that any impact on algal photosynthesis may cause disturbance of cell functioning. The exposure of cells to Al_2O_3, Mn_3O_4, SiO_2 and SnO_2 NPs induced a reduction of Φ_{PSII} (Fig. 7), which indicated a decrease in the light utilization efficiency of PSII of algal cells. In fact, Φ_{PSII} gives a measure of the efficiency at which light absorbed by PSII is used in photochemistry (Baker, 2008). Most likely due to the reduction of the efficiency of photosynthesis, algal cells exposed to the NPs studied should present reduced levels of ATP which, in turn, can be one of the reasons (or the main reason) of algal growth inhibition. A disturbance of photosynthesis was also described in algal cells of *P. subcapitata* exposed for 72 h to CeO_2 or NiO NPs (Rodea-Palomares et al., 2012; Sousa et al., 2018).

The electrons that were no longer used in the photosynthesis (due to the reduction of PSII activity) could induce the production of ROS through the reduction of molecular oxygen (Rutherford and Krieger-Liszkay, 2001). Compatible with this possibility, intracellular accumulation of ROS in algal cells exposed to 72 h-EC_{50} and 72 h-EC_{90} values of Al_2O_3, Mn_3O_4 or SiO_2 NPs was observed (Fig. 6). Our results are in agreement with those of different authors, who reported ROS production in different model cells when exposed to Al_2O_3, Mn_3O_4 or SiO_2 NPs. Thus, it was described that Al_2O_3 NPs caused oxidative stress in the plant *Triticum aestivum* (Yanik and Vardar, 2015, 2018) and in human lymphocytes (Rajiv et al., 2016); Mn_3O_4 NPs induced ROS production in rat alveolar cells (Frick et al., 2011; Urner et al., 2014) and SiO_2 NPs provoked ROS production in lymphocytes (Azimipour et al., 2018), intestinal (Setyawati et al., 2015), lung and human bronchial epithelial cells (Eom and Jinhee Cho, 2011; Manke et al.,

2013).

Two of the main intracellular ROS targets are cell membrane (via oxidation of lipids) and proteins, which can be inactivated through oxidation (Valavanidis et al., 2006). The chronic exposure (up to 6 days) of algal cells to the NPs studied, even at high concentrations, did not cause the perturbation of membrane integrity (Fig. 3B). A similar result was observed with the alga *Scenedesmus obliquus* when exposed to SiO_2 NPs (Liu et al., 2018). In relation to protein oxidation, different mechanisms were described, which includes the oxidation of amino acid residues containing aromatic side chain or sulfhydryl groups (Cecarini et al., 2007). In agreement with this possibility, the reduction of esterase activity (metabolic activity) in algal cells exposed to Al_2O_3, Mn_3O_4 or SiO_2 NPs was observed (Fig. 5), which corresponded to the same NPs that caused the intracellular accumulation of ROS (Fig. 6). A similar effect (inhibition of esterase activity) was observed in alveolar and intestinal cells exposed to Mn_3O_4 NPs (Titma et al., 2016).

5. Conclusions

The five NPs tested were unstable in OECD algal medium (low zeta potential values) and presented tendency to agglomerate. However, these agglomerates were easily dispersed by simple agitation and had a loose structure, which makes very unlikely that the toxicity of these NPs could be due to the entrapment of the algal cells in the NP agglomerates. The NPs studied were poorly soluble in OECD medium. However, the amount of Sn^{4+} leached from the SnO_2 NPs seems to be the main contributor for the toxicity observed by this NP.

Using the algal growth inhibition test, performed with the freshwater alga *P. subcapitata,* and based on the 72 h-EC_{50} values obtained, the hazard of the NPs were categorized as: toxic (Al_2O_3 and SnO_2), harmful (Mn_3O_4 and SiO_2) and not classified/not toxic (In_2O_3).

The study of the impact of the NPs on algal cells using five endpoints (growth, membrane integrity, metabolic activity, photosynthetic activity and intracellular ROS accumulation) revealed that, in the case of Al_2O_3, Mn_3O_4 and SiO_2, the algistatic effect (inhibition of algal growth in the absence of cell death - disruption of cell membrane integrity) can be attributed to the great disturbance of algal physiology: reduction of photosynthetic and metabolic activity and intracellular accumulation of ROS. Probably, the electrons not used in the photosynthesis (due to a reduction of electron flux through PSII) could lead to the induction of ROS, which, in turn, may be in the origin of the reduction of metabolic activity as a consequence of the oxidation of sensitive residues of esterases. The exposure of algal cells to SnO_2 NPs induced the disturbance of the functionality of PSII in the absence of intracellular ROS accumulation or loss of metabolic activity. The reduction of the capacity of algal cells to convert light energy into chemical energy (ATP) may be the cause of the algistatic effect observed.

The results presented herein reinforce the need to study the NPs, in an extended way, using ecologically relevant organisms such as the green alga *P. subcapitata*, in order to provide a systematic characterization of their potential pollutant hazards in the aquatic environment.

Funding information

This work was performed in the framework of the financing by Portuguese Foundation for Science and Technology (FCT) under the scope of the strategic funding of UID/BIO/04469/2019 unit and BioTecNorte operation (NORTE-01-0145-FEDER-000004) funded by the European Regional Development Fund under the scope of Norte2020—Programa Operacional Regional do Norte and LAQV (UID/QUI/50006/2013—POCI/01/0145/FEDER/007265) with financial support from FCT/MEC through national funds and co-financed by FEDER, under the Partnership Agreement PT2020.

Compliance with ethical standards

This article does not contain any studies with human participants or animals performed by any of the authors.

Declaration of Competing Interest

The authors declare that they have no conflict of interest.

Acknowledgments

Cátia A. Sousa gratefully acknowledges the doctoral grant (SFRH/BD/101452/2014) from Portuguese Foundation for Science and Technology (FCT).

Appendix A. Supplementary data

Supplementary material related to this article can be found, in the online version, at doi:https://doi.org/10.1016/j.aquatox.2019.105265.

References

Ahamed, M., Akhtar, M.J., Khan, M.A.M., Alhadlaq, H.A., Aldalbahi, A., 2017. Nanocubes of indium oxide induce cytotoxicity and apoptosis through oxidative stress in human lung epithelial cells. Colloids Surf. B Biointerfaces 156, 157–164.
Andreescu, S., Ornatska, M., Erlichman, J.S., Estevez, A., Leiter, J.C., 2012. Biomedical applications of metal oxide nanoparticles. In: Matijević, E. (Ed.), Fine Particles in Medicine and Pharmacy. Springer, Boston, MA, pp. 57–100.
Aruoja, V., Pokhrel, S., Sihtmae, M., Mortimer, M., Madler, L., Kahru, A., 2015. Toxicity of 12 metal-based nanoparticles to algae, bacteria and protozoa. Environ. Sci. Nano 2, 630–644.
Azimipour, S., Ghaedi, S., Mehrabi, Z., Ghasemzadeh, S.A., Heshmati, M., Barikrow, N., Attar, F., Falahati, M., 2018. Heme degradation and iron release of haemoglobin and oxidative stress of lymphocyte cells in the presence of silica nanoparticles. Int. J. Biol. Macromol. 118, 800–807.
Baker, N.R., 2008. Chlorophyll fluorescence: a probe of photosynthesis in vivo. Annu. Rev. Plant Biol. 59, 89–113.
Cecarini, V., Gee, J., Fioretti, E., Amici, M., Angeletti, M., Eleuteri, A.M., Keller, J.N., 2007. Protein oxidation and cellular homeostasis: emphasis on metabolism. Biochim. Biophys. Acta 1773, 93–104.
Dorsey, J., Yentsch, C.M., Mayo, S., McKenna, C., 1989. Rapid analytical technique for the assessment of cell metabolic-activity in marine microalgae. Cytometry 10, 622–628.
EC, 2008. Classification, labelling and packaging of substances and mixtures, amending and repealing – regulation (EC) nº 1272/2008 of the European Parliament and of the Council of 16 D ecember 2008. Off. J. Eur. Union L353, 1–1355.
ECHA, 2016. Endpoint specific guidance. In: ECHA (Ed.), Guidance on Information Requirements and Chemical Safety Assessment. European Chemicals Agency, Helsinki, Finland.
Eom, H.-J., Jinhee Cho, J., 2011. SiO_2 nanoparticles induced cytotoxicity by oxidative stress in human bronchial epithelial cell, Beas-2B. Environ. Health Toxicol. 26, 1–7.
Frick, R., Muller-Edenborn, B., Schlicker, A., Rothen-Rutishauser, B., Raemy, D.O., Gunther, D., Hattendorf, B., Stark, W., Beck-Schimmer, B., 2011. Comparison of manganese oxide nanoparticles and manganese sulfate with regard to oxidative stress, uptake and apoptosis in alveolar epithelial cells. Toxicol. Lett. 205, 163–172.
Geis, S.W., Fleming, K.L., Korthals, E.T., Searle, G., Reynolds, L., Karner, D.A., 2000. Modifications to the algal growth inhibition test for use as a regulatory assay. Environ. Toxicol. Chem. 19, 36–41.
Genty, B., Briantais, J.M., Baker, N.R., 1989. The relationship between the quantum yield of photosynthetic electron transport and quenching of chlorophyll fluorescence. Biochim. Biophys. Acta 990, 87–92.
Hanaor, D., Michelazzi, M., Leonelli, C., Sorrell, C.C., 2012. The effects of carboxylic acids on the aqueous dispersion and electrophoretic deposition of ZrO_2. J. Eur. Ceram. Soc. 32, 235–244.
Hasegawa, G., Shimonaka, M., Ishihara, Y., 2012. Differential genotoxicity of chemical properties and particle size of rare metal and metal oxide nanoparticles. J. Appl. Toxicol. 32, 72–80.
Hirner, A.V., Flaßbeck, D., 2005. Speciation of silicon. In: Cornelis, R., Crews, H., Caruso, J., Heumann, K.G. (Eds.), Handbook of Elemental Speciation II – Species in the Environment, Food, Medicine and Occupational Health. John Wiley & Sons, Ltd, Chichester, UK, pp. 366–377.
Iler, R.K., 1978. The occurrence, dissolution, and deposition of silica. In: Iler, R.K. (Ed.), The Chemistry of Silica: Solubility, Polymerization, Colloid and Surface Properties, and Biochemistry. John Wiley & Sons, Ltd, New York, USA, pp. 3–115.
Jeong, J., Kim, J., Seok, S.H., Cho, W.S., 2016. Indium oxide (In_2O_3) nanoparticles induce progressive lung injury distinct from lung injuries by copper oxide (CuO) and nickel oxide (NiO) nanoparticles. Arch. Toxicol. 90, 817–828.
Juneau, P., Popovic, R., 1999. Evidence for the rapid phytotoxicity and environmental stress evaluation using the PAM fluorometric method: importance and future application. Ecotoxicology 8, 449–455.

Karunakaran, G., Suriyaprabha, R., Rajendran, V., Kannan, N., 2015. Toxicity evaluation based on particle size, contact angle and zeta potential of SiO_2 and Al_2O_3 on the growth of green algae. Adv. Nano Res. 3, 243–255.
Laurent, S., Boutry, S., Müller, R.N., 2018. Metal oxide particles and their prospects for applications. In: Mahmoudi, M., Laurent, S. (Eds.), Iron Oxide Nanoparticles for Biomedical Applications: Synthesis, Functionalization and Application. Elsevier, Ltd, pp. 3–42.
Liu, Y.H., Wang, S., Wang, Z., Ye, N., Fang, H., Wang, D.G., 2018. TiO_2, SiO_2 and ZrO_2 nanoparticles synergistically provoke cellular oxidative damage in freshwater microalgae. Nanomaterials 8, 1–12.
Machado, M.D., Soares, E.V., 2012. Development of a short-term assay based on the evaluation of the plasma membrane integrity of the alga *Pseudokirchneriella subcapitata*. Appl. Microbiol. Biotechnol. 95, 1035–1042.
Machado, M.D., Soares, E.V., 2013. Optimization of a microplate-based assay to assess esterase activity in the alga *Pseudokirchneriella subcapitata*. Water Air Soil Pollut. 224, 1–9.
Machado, M.D., Soares, E.V., 2016. Short- and long-term exposure to heavy metals induced oxidative stress response in *Pseudokirchneriella subcapitata*. Clean Soil Air Water 44, 1578–1583.
Manke, A., Wang, L., Rojanasakul, Y., 2013. Mechanisms of nanoparticle-induced oxidative stress and toxicity. Biomed. Res. Int. 2013, 1–15.
Manzo, S., Buono, S., Rametta, G., Miglietta, M., Schiavo, S., Di Francia, G., 2015. The diverse toxic effect of SiO_2 and TiO_2 nanoparticles toward the marine microalgae *Dunaliella tertiolecta*. Environ. Sci. Pollut. Res. 22, 15941–15951.
Nanotech, 2015. Aluminium oxide: forecast from 2010 to 2025. Nanoparticles. Future Markets Inc., Edinburgh.
Ng, A.M.C., Guo, M.Y., Leung, Y.H., Chan, C.M.N., Wong, S.W.Y., Yung, M.M.N., Ma, A.P.Y., Djurisic, A.B., Leung, F.C.C., Leung, K.M.Y., Chan, W.K., Lee, H.K., 2015. Metal oxide nanoparticles with low toxicity. J. Photochem. Photobiol. B 151, 17–24.
OECD, 2011. Test Nº 201: Freshwater Alga and Cyanobacteria, Growth Inhibition Test. OECD Guidelines for the Testing of Chemicals. Section 2. OECD Publishing, Paris. https://doi.org/10.1787/9789264069923-en.
Rajiv, S., Jerobin, J., Saranya, V., Nainawat, M., Sharma, A., Makwana, P., Gayathri, C., Bharath, L., Singh, M., Kumar, M., Mukherjee, A., Chandrasekaran, N., 2016. Comparative cytotoxicity and genotoxicity of cobalt (II, III) oxide, iron (III) oxide, silicon dioxide, and aluminium oxide nanoparticles on human lymphocytes in vitro. Hum. Exp. Toxicol. 35, 170–183.
Rodea-Palomares, I., Gonzalo, S., Santiago-Morales, J., Leganes, F., Garcia-Calvo, E., Rosal, R., Fernandez-Pinas, F., 2012. An insight into the mechanisms of nanoceria toxicity in aquatic photosynthetic organisms. Aquat. Toxicol. 122, 133–143.
Rogers, N.J., Franklin, N.M., Apte, S.C., Batley, G.E., Angel, B.M., Lead, J.R., Baalousha, M., 2010. Physico-chemical behaviour and algal toxicity of nanoparticulate CeO_2 in freshwater. Environ. Chem. 7, 50–60.
Rutherford, A.W., Krieger-Liszkay, A., 2001. Herbicide-induced oxidative stress in photosystem II. Trends Biochem. Sci. 26, 648–653.
Sadiq, I.M., Pakrashi, S., Chandrasekaran, N., Mukherjee, A., 2011. Studies on toxicity of aluminum oxide (Al_2O_3) nanoparticles to microalgae species: *Scenedesmus* sp and *Chlorella* sp. J. Nanopart. Res. 13, 3287–3299.
Setyawati, M.I., Tay, C.Y., Leong, D.T., 2015. Mechanistic investigation of the biological effects of SiO_2, TiO_2, and ZnO nanoparticles on intestinal cells. Small 11, 3458–3468.
Sousa, C.A., Soares, H.M.V.M., Soares, E.V., 2018. Toxic effects of nickel oxide (NiO) nanoparticles on the freshwater alga *Pseudokirchneriella subcapitata*. Aquat. Toxicol. 204, 80–90.
Tarpey, M.M., Wink, D.A., Grisham, M.B., 2004. Methods for detection of reactive metabolites of oxygen and nitrogen: in vitro and in vivo considerations. Am. J. Physiol. Regul. Integr. Comp. Physiol. 286, R431–R444.
Tian, Z.-Y., Kouotou, P.M., Bahlawane, N., Ngamou, P.H.T., 2013. Synthesis of the catalytically active Mn_3O_4 spinel and its thermal properties. J. Phys. Chem. C 117, 6218–6224.
Titma, T., Shimmo, R., Siigur, J., Kahru, A., 2016. Toxicity of antimony, copper, cobalt, manganese, titanium and zinc oxide nanoparticles for the alveolar and intestinal epithelial barrier cells in vitro. Cytotechnology 68, 2363–2377.
Urner, M., Schlicker, A., Z'Graggen, B.R., Stepuk, A., Booy, C., Buehler, K.P., Limbach, L., Chmiel, C., Stark, W.J., Beck-Schimmer, B., 2014. Inflammatory response of lung macrophages and epithelial cells after exposure to redox active nanoparticles: effect of solubility and antioxidant treatment. Environ. Sci. Technol. 48, 13960–13968.
US-EPA, 2002. Short-Term Methods for Estimating the Chronic Toxicity of Effluents and Receiving Waters to Freshwater Organisms, 4th ed. Environmental Protection Agency, Washington, DC, pp. 1–350 EPA-821-R-302-013.
Valavanidis, A., Vlahogianni, T., Dassenakis, M., Scoullos, M., 2006. Molecular biomarkers of oxidative stress in aquatic organisms in relation to toxic environmental pollutants. Ecotoxicol. Environ. Saf. 64, 178–189.
Vranic, S., Shimada, Y., Ichihara, S., Kimata, M., Wu, W., Tanaka, T., Boland, S., Tran, L., Ichihara, G., 2019. Toxicological evaluation of SiO_2 nanoparticles by zebrafish embryo toxicity test. Int. J. Mol. Sci. 20, 1–12.
Wang, Y.L., Ding, L., Yao, C.J., Li, C.C., Xing, X.J., Huang, Y.A., Gu, T.J., Wu, M.H., 2017. Toxic effects of metal oxide nanoparticles and their underlying mechanisms. Sci. China Mat. 60, 93–108.
Yanik, F., Vardar, F., 2015. Toxic effects of aluminum oxide (Al_2O_3) nanoparticles on root growth and development in *Triticum aestivum*. Water Air Soil Pollut. 226, 1–12.
Yanik, F., Vardar, F., 2018. Oxidative stress response to aluminum oxide (Al_2O_3) nanoparticles in *Triticum aestivum*. Biologia 73, 129–135.